ACOUSTIC EMISSION OF SIC/SIC COMPOSITE DURING TENSILE TEST AND STATIC FATIGUE AT INTERMEDIATE TEMPERATURE AFTER IMPACT DAMAGE.

P. Reynaud, N. Godin, M. Picard, M. R'Mili, G.Fantozzi
INSA-Lyon, Laboratoire MATEIS, Villeurbanne, France

pascal.reynaud@insa-lyon.fr, nathalie.godin@insa-lyon.fr, martin.picard@insa-lyon.fr, mohamed.rmili@insa-lyon.fr, gilbert.fantozzi@insa-lyon.fr

Keywords: damage sensitivity, fatigue tests, acoustic emission, lifetime prediction

Abstract

This paper discusses the tensile resistance of an impact-damaged SiC/SiC based ceramic composite. As-received and impact-damaged specimens were subjected to static fatigue tests at 650°C and 450°C. Damage induced during the tensile and fatigue tests was characterized using unloading-reloading cycles and evolution of linear density of events of acoustic emission (AE). Results have shown the material impact insensitivity while the analysis of AE signals has demonstrated its efficiency to properly investigate damage evolution in the impacted specimens. The approach for the investigation of lifetime is based on the determination of energy released and identification of a critical point in energy release during mechanical test. An equivalent energy of AE sources is defined, which is calculated for each AE event using the signal energy received at two sensors. An indicator based on AE energy allows identifying a characteristic time at 55 % of rupture time. So beyond this characteristic point, the criticality can be modelled with a power-law in order to evaluate time to failure.

1. Introduction

Due to low weight/mechanical ratio and high temperature strength, ceramic matrix composites (CMCs) are very attractive candidates for civil aircrafts applications. For these applications, resistance to foreign object damage (FOD) is a key issue to insure structural reliability in service. In the literature, a few authors have investigated the FOD response of 2D woven CMC [1-5]. They have shown that low energy impact was equivalent to quasi-static indentation and that a conical damage zone was created.

Meanwhile, investigations by Ogi *et al.* [6] and Herb *et al.* [7] on 3D woven CMC have shown that tri-dimensional fibre architectures prevent the material from delamination so that the damaged cone remains limited and well delineated. After indentation (*i.e.* ballistic or quasi-static impact tests), residual strengths were measured using tensile or flexural tests at room temperature.

Few works on the effect of impact damage on composite lifetime under fatigue at elevated temperature have been reported. Recently, Verrilli *et al.* [5]. have performed cyclic fatigue tests on 2D cross ply SiC/SiC composite at 1316°C after impact tests at 1200°C. They have observed that lifetime decreases tremendously with increasing impact energy. After high energy impact damage the average lifetime was 40 times as small as that obtained after low energy impact tests. However, impact damage evolution during fatigue has not been studied in real time.

This paper investigates the evolution of impact damage during fatigue at high temperature on a 3D SiC/SiC composite using acoustic emission signals and the sensitivity to impact damage. Acoustic emission data were post-treated using homemade software that determines the spatial distribution of

Excerpt from ISBN 978-3-00-053387-7

AE events during the tests. As-fabricated and impact-damaged specimens were tested at room and at intermediate temperatures (*i.e.* 450°C and 650°C).
The approach in order to investigate the remaining lifetime, proposed in the present paper, is based on determination of energy released at AE sources [8] and identification of a critical point in energy release using the coefficient of emission R_{AE} [9].

2. Experimental procedure

2.1. Material and specimen preparation

The SiC/SiC composite investigated (manufactured by Heraklès - SAFRAN Group (Bordeaux, France)) was made of an interlock preform with a self-healing [Si-B-C] matrix. The fibres were coated by a PyC layer deposited via chemical vapour infiltration. Such a 3D fibrous preform (Guipex® preform) improves the through thickness properties. Yarns contain 500 SiC Nicalon fibres. The fibre volume fraction was between 35% and 40% and the porosity volume fraction was around 12%. A barrier coating protected the surface of samples against oxidation.

Rectangular test specimens were machined out of 1.8 mm thick panels: specimens' dimensions were 24 mm in width and 200 mm in length. Impact damage was generated by quasi-static indentation by Herb *et al.* [7]. A hemispherical steel punch with a 9 mm diameter was used.

Fig. 1 shows the cone crater that had been created. Breakage of fibre bundles was observed on back side (Fig. 1a), as well as on impact side (Fi. 1b). On impact side, the sample displayed a neat circular mark. Images of impact and back sides were post-treated using the Image J software, in order to measure cone area on each side of samples. It was found to be about 33 mm^2 on the front side which corresponds to an equivalent hole with a diameter of 6.5 mm. On the back side, the damaged area was about 85 mm^2 which could be assimilated to an equivalent hole with a 10.5 mm diameter. The cone crater was sharply delineated, which can be attributed to the 3D fibrous architecture of material and the resulting absence of delamination.

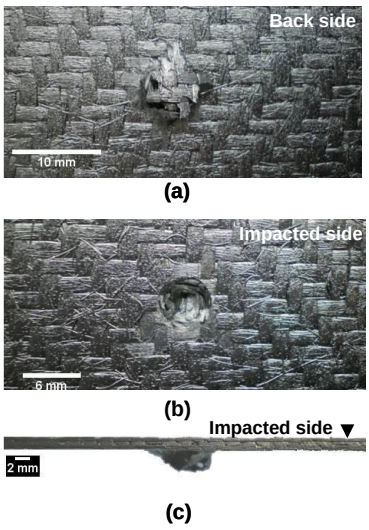

Figure 1. Optical photographs of the SiC/SiC specimens after quasi static indentation: (a) back side (d_i^B= 10.5 mm) (b) impacted side (d_i^F = 6.5 mm) (c) thickness view.

Excerpt from ISBN 978-3-00-053387-7

2.2. Post-indentation mechanical testing

Static fatigue and tensile experiments were performed using a 25kN uniaxial pneumatic tensile loading machine with one direction of fibres parallel to the loading direction. Specimen elongation was measured using an extensometer (gauge length = 32 mm) with ceramic rods.

Static fatigue tests were carried out at 450°C and 650°C under air, with uniform temperature in the gauge length. Specimens were heated up to the test temperature at a rate of 20°C/min. The load was applied after 2 hours, when the gauge length was expected to be at the test temperature. During the static fatigue tests, specimens were first loaded at a constant rate of 1200 N/min up to the test load corresponding to 80 MPa, close to the elastic limit of composite or to 125 MPa. For all the tests, damage was characterized using periodical unloading-loading cycles (every 12 hours during the static fatigue tests) and also acoustic emission signals.

2.3. Acoustic emission monitoring

AE was monitored using a MISTRAS 2001 data acquisition system (Euro Physical Acoustics). Two MICRO-80 sensors were positioned directly on the specimen, inside the grips, using vacuum grease with a medium viscosity as a coupling agent. Acquisition parameters were set as follows: pre-amplification 40 dB, threshold 36 dB, peak definition time 50 µs, hit definition time 100 µs, hit lockout time 1000 µs. AE signal parameters (amplitude, energy, duration, counts, location…) as well as time, load and strain were measured in real time by the data acquisition system. Since two sensors only were used, the longitudinal positions of AE origins were determined (fig. 3a).

AE sources locations were derived using AE wave velocity, that was measured using a pencil lead break procedure: 9100 m/s for both the as-fabricated and the impact- damaged specimens. Morscher *et al.* [10] showed that in ceramic matrix composites wave velocity decreases with increasing stress induced damage. Wave velocity value was corrected using the attenuation coefficient γ:

$$\gamma = \sqrt{\frac{E}{E_0}} \quad (1)$$

where E is the secant elastic modulus determined from unloading-reloading hysteresis loops and E_0 is the initial elastic modulus. AE data were post-treated using dedicated software, which provides linear density along specimen axis of acoustic events during the tests. This analysis of acoustic emission is non-trivial. It is useful to identify the most active zones during the tests.

2.4. Determination of the source energy [8]

It is generally accepted that the energy of an AE signal is a part of the energy released at the source. The recorded AE signal energy is affected by distance of wave propagation, energy attenuation due to damage, coupling between sensor and material, and by sensor frequency response. The effects of attenuation due to propagation distance can be eliminated by combining AE signals energies recorded by sensors. The influence of coupling may lead to a different amount of energy received by each sensor even for a source located at equal distance. Hence, by comparing the amount of energy received at each sensor from any source located at mid-distance, recorded AE energies can be calibrated [8]. For comparison, amounts of energy associated with sources located within a ± 5 mm distance from the middle of gauge length were studied. In order to exclude the effects of damage, only the beginning of initial loading (strain lower than 0.1%) was considered. The above-described space-time interval for comparison was denoted *st* (standardization domain). Comparison was then performed using the distribution functions of amounts of energy received by each sensor.

It can be stated that both sensors being at the same distance from the standardization domain, they should receive statistically the same proportion of signals energy. This means that both distribution functions should be superimposed when considering sources located in the standardization domain.

Excerpt from ISBN 978-3-00-053387-7

The distribution functions were thus centered and scaled, which gives for a signal initiated from a source *n* and received by sensor 1:

$$E_1^*(n) = \left[E_1(n) - med_{st,1}\right] / S_{st,1} \qquad (1)$$

where $med_{st,1}$ and $S_{st,1}$ are the median and standard deviations values of the amount of energy received at sensor 1 for sources located in the standardization domain (*st*). To make further analysis easier, values were standardized as follows:

$$E_1^{'}(n) = \left[E_1^*(n) - \min_{st}\left\{E_1^*, E_2^*\right\}\right] / \left[\max_{st}\left\{E_1^*, E_2^*\right\} - \min_{st}\left\{E_1^*, E_2^*\right\}\right] \qquad (2)$$

where minimum (min_{st}) and maximum (max_{st}) values were calculated considering the values of E^* at sensors 1 and 2 for all the sources located in the standardization domain (*st*).

The source energy is then defined as the square root of the product of the energy amounts received at both sensors for each source:

$$K(n) = \sqrt{E_1^{'}(n) \times E_2^{'}(n)} \qquad (3)$$

where L is the distance between sensors, $L = x_1 + x_2$.

Thus, the evolution of elastic energy released by analysing the energy of AE events may be investigated. The coefficient of emission R_{AE} is defined as the increment of energy ΔE recorded during an increment of time Δt, divided by the total energy emitted during the initial loading of the sample:

$$R_{AE}(t) = \frac{1}{\mathrm{E}_{\mathrm{loading}}} \frac{\Delta \mathrm{E}}{\Delta \mathrm{t}} \qquad (4)$$

where $E_{loading}$ is the cumulative AE energy for all the signals recorded during the initial loading up to the nominal load of the test, ΔE is the cumulative AE energy for all signals recorded during the interval [t; t + Δt].

3. Results and discussion

During the tensile tests, the impacted specimens failed from the mid-plane whereas the as-fabricated samples failed from the upper or lower parts of the gauge length. Figure 2a shows typical tensile curves. For both the as-fabricated and the impact-damaged specimens, the stresses were determined from the net-section of samples:

$$\sigma = \frac{F}{(w-a)b} \qquad (5)$$

where F is the force on specimen, w is specimen width, a is the average diameter of crater, b = 1.1 mm is specimen effective thickness. As shown by Figure 2a, for all the samples, the tensile response was essentially non-linear, beyond the proportional limit, as a result of stress-induced matrix cracking. The two impacted specimens exhibited higher stresses (or smaller deformations) and a slightly smaller ultimate strength compared to as-fabricated specimens (Figure 2a): ultimate strength was 80% of the reference, whereas strain-to-failure was reduced by 50%.

To evaluate the impact damage sensitivity strength data were plotted with respect to average cone diameter size according the classical equation for notch sensitivity, which indicates that the stress at failure at hole tip is equal to the strength of specimen without hole:

Excerpt from ISBN 978-3-00-053387-7

$$\sigma_R(a) = \sigma_R(a=0)(1-\frac{a}{w}) \quad (6)$$

where a is average diameter of cone (figure 2b), σ_R is the failure stress given by F/wb.

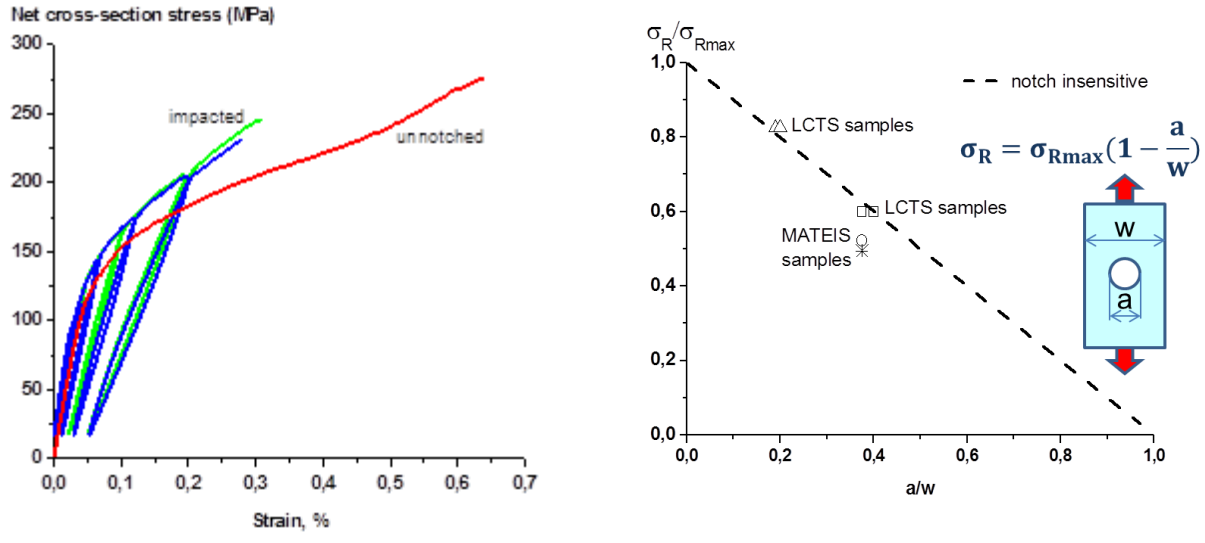

a) b)

Figure 2. (a) Tensile behaviour of impact-damaged and as-fabricated specimens. (b) Post-indentation relative strength of the specimens versus the relative diameter of damage cone (comparison with results from Herb *et al.* [7]).

Figure 2a shows that equation (3) fits the strength data which indicates that the material is insensitive to impact damage. It means that there is no significant stress concentration induced by the presence of the impact cone. The σ_R strength dependence on a results instead from reduction in specimen section.

Figures 3a and 3b show the evolution of linear density of acoustic events during monotonous loading. It can be noticed that acoustic emission was very active in the zone of impact (*i.e.* between the dotted lines) for both samples at the beginning of loading (*i.e.* for strain level values between 0 and 0.10%). Failure did not occur under these strains but much later under larger deformation. Instead, under these larger strains, the AE activity in the impact area slowed down whereas it increased progressively in other parts of specimen, but looked quite homogeneous as load increased indicative of diffuse stress induced damage. These results are consistent with impact damage insensitivity previously indicated. They indicate that the impacted specimens experience damage exactly like the as-received specimens under tensile load: stress driven diffuse matrix cracking and, in a second step, fibre failures.

For the static fatigue tests conducted at 80 MPa and at 450°C and 650°C, these specimens did not fail even after 1000 hours. Thus, the fatigue tests were interrupted and the tensile residual strength was measured at room temperature. Residual strength was also measured using tensile tests at room temperature. Figure 4 compares initial and residual strengths for both as-fabricated specimens and impact-damaged specimens.

Excerpt from ISBN 978-3-00-053387-7

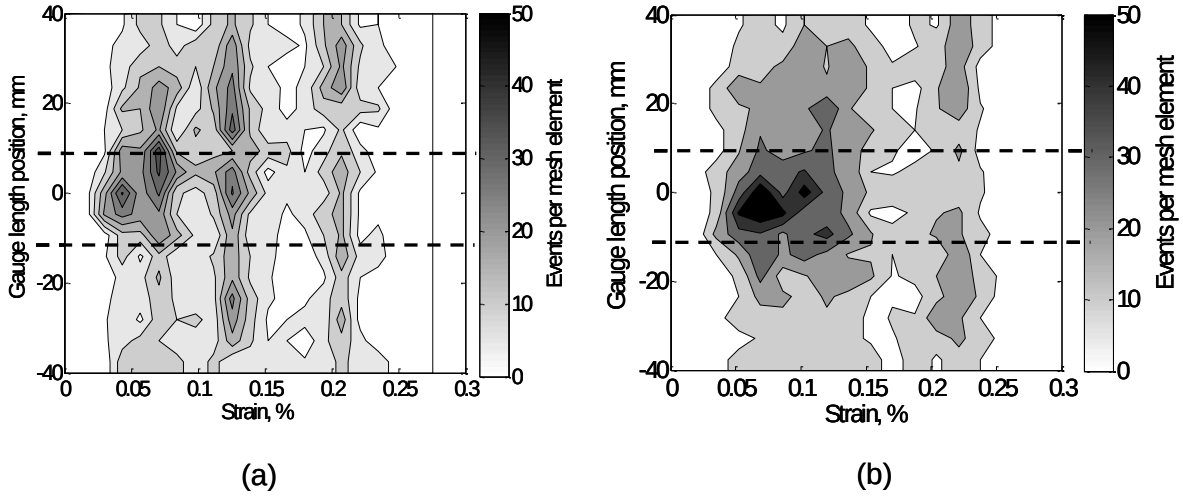

Figure 3. Evolution of linear densities of acoustic events along specimen axis during tensile tests at room temperature for the two impacted specimens (a) Impacted sample1. (b) Impacted sample2. The dotted lines bound the damage cone area.

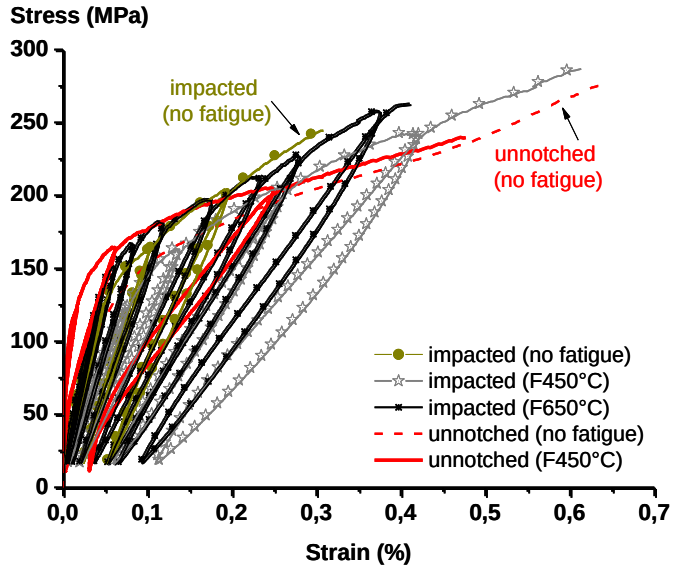

Figure 4. Comparison of the initial and residual tensile behaviour at room temperature of as-fabricated and impact-damaged specimens.

Though the tensile behaviour exhibits some variation (probably a material feature), the stress-strain curves highlight three important features. First, for both the as-fabricated and the impact-damaged specimens, the residual strengths were not significantly affected by fatigue tests at intermediate temperature. Second, though material protection by matrix healing was not effective at 450°C, residual strength of the impacted specimens after 1000 hours of static fatigue was unchanged whatever the test temperature. Third, the residual failure stresses and strains for the impact-damaged specimens were close to those obtained on the as-fabricated samples after fatigue. These features again indicate that under current experimental conditions the SiC/SiC composite fatigue behaviour was impact damage less sensitive.

The evolution [9] of R_{AE} coefficient versus time is given (Fig. 5a) in log scale for different applied stresses for undamaged specimens. In both cases, R_{AE} decreases first, down to a minimum value, and then increases up to the failure of the composite. On average, the minimum of R_{AE} appeared at 55% of the rupture time. R_{AE} allowed also identify a characteristic time. The minimum of the coefficient R_{AE}

Excerpt from ISBN 978-3-00-053387-7

indicates the beginning of the critical damage phase and provides an estimate of the remaining lifetime. The restart of activity prior to final rupture may be attributed to the avalanche fibres ruptures, controlled by the oxidation of fibres and by the recession of interfaces. In order to confirm this hypothesis, this coefficient is calculated for several damage mechanisms identified with clustering analysis of AE data [11]. The coefficients R_{AE} obtained for the two classes A and B go through a minimum, contrary to those of classes C and D (Fig.5b). It may be noticed that the minimum of the coefficient R_{AE} is observed only for clusters A and B corresponding to fibers breaks during the second part of the test around 65 % of the rupture time. The coefficient R_{AE} (Fig 6) was also calculated for the impacted specimen, and the minimum value for the coefficient RAE was only observed for tests conducted until failure around 50 % of rupture time. These results are consistent with impact damage insensitivity previously indicated.

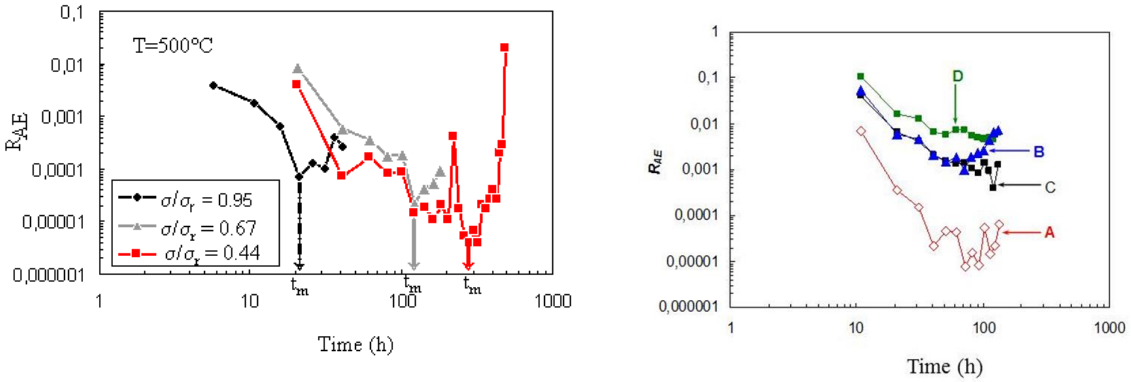

Fig. 5 : a) Evolution of the R_{AE} coefficient during the static load hold for several tests on SiC_f/[Si-B-C] composites b) Evolution of the R_{AE} coefficient during the static load hold for the different clusters denoted A, B, C and D.

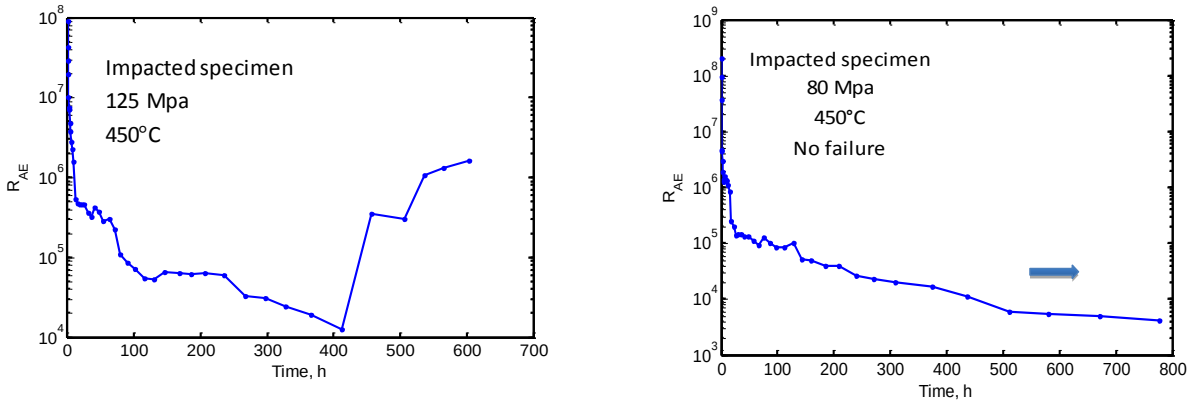

Fig. 6: Evolution of the R_{AE} coefficient during the static load hold on impacted specimen a) test conducted until to ultimate failure b) no failure

4. Conclusion

This paper investigated the effect of impact damage on SiC/SiC composite tensile behaviour at room temperature and static fatigue resistance at two intermediate temperatures (450°C and 650°C). An original homemade software for post-treatment of AE signals from specimens gauge length during tests provided maps of linear density of acoustic events. These maps imaged damage during the tests. They showed that emission was intense near the impact cone at beginning of tests only. Specimens

Excerpt from ISBN 978-3-00-053387-7

failed under larger strains. Their subsequent response was comparable to the non-linear mechanical behaviour of as-fabricated specimens. This observation illustrates the insensitivity to damage of this material, which is consistent with the notch insensitivity of long fibers reinforced composites. The indicators (R_{AE}) allows identifying a characteristic time at 55 % of rupture time for the undamaged specimen and also for the impacted. So beyond this characteristic point, the criticality can be modelled with a power-law in order to evaluate time to failure. Future work will focus on the use of Benioff law as a predictive model on impacted sample.

Acknowledgments

The authors gratefully acknowledge DGCIS, Conseil Régional d'Aquitaine, DGAC, DGA, CNRS and Aerospace Valley for supporting this work in the frame of the program ARCOCE: "Arrière-Corps Composite Ceramique, Ceramic Matrix Composites for Exhausts", and particularly P. Diss (SAFRAN, SNECMA Propulsion Solide) for fruitful discussions.

References

[1] Bhatt RT, Choi SR, Cosgriff LM, Fox DS, Lee KN. Impact resistance of environmental barrier coated SiC/SiC composites. Mater Sci Eng A 2008; 476:8–19.

[2] Bhatt RT, Choi SR, Cosgriff LM, Fox DS, Lee KN. Impact resistance of uncoated SiC/SiC composites. Mater Sci Eng A 2008; 476:20–8.

[3] Choi SR. Foreign object damage phenomenon by steel ball projectiles in a SiC/SiC ceramic matrix composites at ambient and elevated temperatures. J Am Ceram Soc 2008; 91:2963–8.

[4] Choi SR, Alexander DJ, Kowalik RW. Foreign object damage in an oxide/oxide composite at ambient temperature. J Eng Gas Turb Power 2009; 131:021301-1–0212301-6

[5] Virelli M, Impact Behavior of a SiC/SiC Composite at an Elevated Temperature, In: Proceedings of the 7th International Conference on High Temperature Ceramic Matrix Composites (HTCMC-7), editors Krenkel W and Lamon J, pp. 519–530, Bayreuth, Germany, 20–22 September 2010.

[6] Ogi K, Okabe T, Takahashi M, Yashiro S, Yoshimura A, Ogasawara T. Experimental characterization of high-speed impact damage behaviour in a three-dimensionally woven SiC/SiC composite. Composites: Part A 2010; 41:489–498.

[7] Herb V *et al.* Damage assessment of thin SiC/SiC composite plates subjected to quasi-static indentation loading. Composites: Part A 2010, doi:10.1016/j.compositesa. 2010.08.004

[8] Maillet E., Godin N., R'Mili M., Reynaud P., Lamon J., Fantozzi G., Indicators of the critical behavior of Ceramic Matrix Composites for rupture time prediction during fatigue tests at intermediate temperatures, *Composites Science and Technology*, 72 pp 1001–1007, 2012.

[9] Momon S, Moevus M, Godin N, R'Mili M, Reynaud P, Fantozzi G, Fayolle G, Acoustic emission and lifetime prediction during static fatigue tests on ceramic-matrix-composite at high temperature under air Composites: Part A, 2010; 41, 913-918.[9].

[10] Morscher, G.N., 1998. Modal acoustic emission of damage accumulation in a woven SiC/SiC composite. Comp. Sci. Tech, 1999, 59, 687-697.

[11] Moevus M, Rouby D, Godin N, R'Mili M, Reynaud P, Fantozzi G, Fayolle G, Analysis of damage mechanisms and associated acoustic emission in two SiC_f/[Si–B–C] composites exhibiting different tensile behaviours. Part II: Unsupervised acoustic emission data clustering, Comp. Sc. and Tech., 2008, 68, 1250-1257.

Excerpt from ISBN 978-3-00-053387-7

Excerpt from ISBN 978-3-00-053387-7